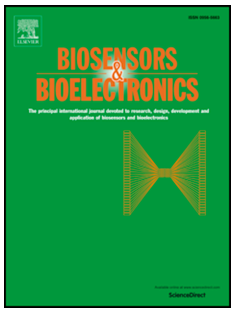

Gold nanocap-supported upconversion nanoparticles for fabrication of a solid-phase aptasensor to detect ochratoxin A

Kihyeun Kim, Eun-Jung Jo, Ki joong Lee, Jiyoon Park, Gun Young Jung, Yong-Beom Shin, Luke P. Lee, Min-Gon Kim

PII: S0956-5663(19)30964-9

DOI: https://doi.org/10.1016/j.bios.2019.111885

Reference: BIOS 111885

To appear in: *Biosensors and Bioelectronics*

Received Date: 21 October 2019

Revised Date: 12 November 2019

Accepted Date: 13 November 2019

Please cite this article as: Kim, K., Jo, E.-J., Lee, K.j., Park, J., Jung, G.Y., Shin, Y.-B., Lee, L.P., Kim, M.-G., Gold nanocap-supported upconversion nanoparticles for fabrication of a solid-phase aptasensor to detect ochratoxin A, *Biosensors and Bioelectronics* (2019), doi: https://doi.org/10.1016/j.bios.2019.111885.

CRediT author statement

Kihyeun Kim: Conceptualization, Methodology, Validation, Formal Analysis, Investigation, Visualization, Writing – Original Draft, Writing – Review & Editing

Eun-Jung Jo: Methodology, Formal Analysis, Investigation, Writing – Original Draft

Ki joong Lee: Methodology, Formal Analysis, Investigation

Jiyoon Park: Methodology, Investigation

Gun Young Jung: Investigation, Writing – Review & Editing

Yong-Beom Shin: Formal Analysis, Investigation, Writing – Review & Editing

Luke P. Lee: Conceptualization, Writing – Review & Editing, Funding acquisition, Supervision, Project Administration

Min-Gon Kim: Conceptualization, Writing – Review & Editing, Funding acquisition, Resources, Supervision, Project Administration

Gold nanocap-supported upconversion nanoparticles for fabrication of a solid-phase aptasensor to detect ochratoxin A

Kihyeun Kim[a], *Eun-Jung Jo*[a], *Ki joong Lee*[b], *Jiyoon Park*[c], *Gun Young Jung*[c], *Yong-Beom Shin*[b,d], *Luke P. Lee*[e]* *and Min-Gon Kim*[a]*

[a]Department of Chemistry, Gwangju Institute of Science and Technology (GIST), Gwangju 61005, Republic of Korea

[b]Bionanotechnology Research Center, Korea Research Institute of Bioscience and Biotechnology (KRIBB), 125 Gwahak-ro, Yuseong-gu, Daejeon 34141, Republic of Korea

[c]School of Materials Science and Engineering, Gwangju Institute of Science and Technology (GIST), Gwangju 61005, Republic of Korea

[d]BioNano Health Guard Research Center, 125 Gwahak-ro, Yuseong-gu, Daejeon 34141, Republic of Korea

[e]Department of Bioengineering, Department of Electrical Engineering and Computer Science, and Biophysics Graduate Program, University of California, Berkeley, California 94720, United States

***Corresponding authors**

Email: mkim@gist.ac.kr, tel.: +82-62-715-3330, fax: +82-62-715-2887 (Min-Gon Kim);
email: lplee@berkeley.edu, tel.: +1-510-642-5855, fax: +1-510-642-5835 (Luke P. Lee)

ABSTRACT

Solid-phase, single-step biosensors are crucial for the development of portable, reusable, and convenient biosensors, otherwise known as point-of-care (POC) testing. Although high-performance single-step biosensors based on the principle of Förster resonance energy transfer (FRET) and using upconversion nanoparticles (UCNPs) functionalized with aptamers have been suggested as easy-to-use platforms, they lack portability and reusability when used for solution-phase biosensing. In this study, we describe a solid-phase, single-step aptasensor that showed higher performance than those of solution-phase aptasensors, as well as promising reusability. The solid-phase, single-step aptasensor was developed based on Au nanocap-supported UCNPs (Au/UCNPs), which were partially embedded in a solid substrate (e.g. polydimethylsiloxane, PDMS). The Au nanocaps allowed the UCNPs to emit upconverted light only from the restricted areas of the UCNPs, i.e., where they were not covered by the nanocaps and PDMS. Functionalization of an aptamer labeled with a quencher on the restricted area enabled the effective quenching of upconverted light from Au/UCNP via FRET after target (ochratoxin A, OTA) detection. The solid-phase, single-step aptasensor showed a linear range of 0.1–1000 ng mL^{-1} and limit of detection of 0.022 ng mL^{-1} within 30 min toward OTA. Furthermore, reusability of the solid-phase aptasensor was evaluated for three cycles of detection and regeneration, establishing its apparent reusability via heat treatment. Hence, such solid-phase, single-step aptasensors pave the path to the development of a portable and reusable biosensor platform for POC testing.

KEYWORDS: Upconversion nanoparticles, solid phase, single step, biosensor, Au nanocap, aptasensor, ochratoxin A

1. INTRODUCTION

Portable and easy-to-use biosensors are highly important for future healthcare systems that are individual-centered, also known as point-of-care (POC), rather than laboratory- or hospital-centered (Gubala et al., 2012; Vashist et al., 2015; Nayak et al., 2017; Wood et al., 2019). Based on rapid advances in nanomaterial-based technology, various designs for nanoparticle–bioreceptor conjugates dispersed in solution have led to the development of sensitive biosensor platforms that are potentially applicable for POC (Luppa et al., 2011; Quesada-González and Merkoçi, 2018; Samorì and Biscarini, 2018; Ye et al., 2018). In particular, upconversion nanoparticles (UCNPs) have attracted much attention as strong candidates for such conjugates because they can be excited by near-infrared light without photodamage or matrix effects and emit highly stable visible light (Zheng et al., 2015; Sedlmeier and Gorris, 2015; Gu and Zhang, 2018; Ye et al., 2014; Xu et al., 2014; Jo et al., 2018). To take advantage of these properties, the functionalization of bioreceptors on UCNPs has been explored to develop target-specific and high-performance biosensor platforms based on quenching of the upconversion luminescence (UCL) of UCNPs in the presence of target molecules via Förster resonance energy transfer (FRET) (Ye et al., 2014; Xu et al., 2014; Jo et al., 2018). Despite the high sensitivities achieved by nanoparticle–bioreceptor conjugates dispersed in solution, the development of biosensors for POC testing remains a challenge due to their poor portability, the aggregation of the conjugates, reusability issues, and their complexity of use.

Solid-phase, single-step biosensors are regarded as strong candidates to solve such challenges, as the immobilization of nanoparticles, bioreceptors, and their conjugates on solid substrates provides a highly portable reusable platform, and avoids the issue of nanoparticle aggregation (Guan et al., 2015; Han et al., 2017). In addition, single-step biosensors are facile to

employ, as no centrifuge equipment is required for the washing steps, and the process tends to be less time-consuming (Jo et al., 2018). In the context of single-step biosensors, our group has recently reported a conjugate (i.e., a UCNP functionalized with quencher (organic dye)-labeled aptamers) that enables highly sensitive single-step detection of small molecules, and is a highly convenient biosensor platform for individual users because of its single-step procedure for target detection (Jo et al., 2018). Nevertheless, such biosensors based on conjugates dispersed in solution (also known as solution-phase biosensors) have considerable limitations in terms of the development of POC biosensors as they do not take advantage of solid-phase biosensors.

Although there have been a few studies on the immobilization of UCNPs on solid substrates and subsequent functionalization of bioreceptors onto the UCNPs to develop platforms for solid-phase biosensors (Doughan et al., 2014; Doughan et al., 2015), solid-phase, single-step biosensors with sensitivities comparable to solution-phase ones have not yet been reported. Therefore, biosensors satisfying solid-phase and single-step are highly demanded for the development of future POC biosensors.

In this study, we demonstrated solid-phase, single-step biosensors based on Au nanocap-supported UCNPs (Au/UCNPs) partially embedded in a solid substrate (e.g., polydimethylsiloxane, PDMS), where quencher-labeled aptamers were functionalized on the UCNPs to detect ochratoxin A (OTA). The Au/UCNPs can emit strong and directional upconverted light from only the restricted surface of the Au/UCNPs that is not covered by the Au nanocap (**Scheme 1**); this strong and directional upconversion emission from the restricted area of the UCNPs stems from plasmon enhancement of the UCL caused by the Au nanocap (Bang et al., 2017; Hinamoto et al., 2017). Then, quencher-labeled aptamers were covalently functionalized on the restricted surface of Au/UCNPs, where the UCNPs were not covered by

the Au nanocap. Thus, the quencher-labeled aptamers could effectively quench the directionally emitted light from the Au/UCNPs via FRET depending on the OTA concentration, which showed comparable and even higher sensitivity to that of solution-phase biosensors. The higher sensitivity is expected possibly because of enhanced FRET efficiency originating from increased UCL of UCNPs and/or plasmon-assisted FRET by Au nanocap. Finally, the solid-phase, single-step aptasensors were successfully applied as reusable biosensors via heat treatment. Hence, the fabrication of aptamer-functionalized Au/UCNPs on PDMS could pave the way for the development of solid-phase, single-step biosensors.

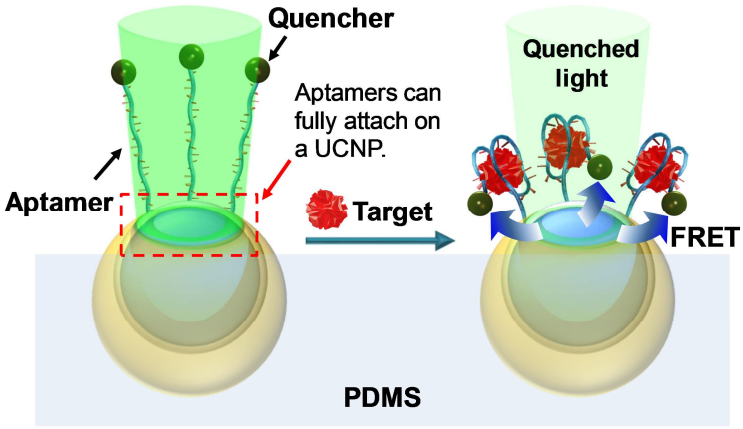

Scheme 1. Working principle of an aptamer (labeled with quenchers)-functionalized Au nanocap-supported UCNP (Au/UCNP).: The aptamer can only attach in the regions where the UCNP is not covered by Au, which results in effective quenching of UCL from Au/UCNP in the presence of OTA.

2. EXPERIMENTAL SECTION

2.1. Materials

Yttrium(III) acetate hydrate ($Y(CH_3COO)_3 \cdot xH_2O$, 99.9% metals basis), ytterbium(III) acetate hydrate ($Yb(CH_3COO)_3 \cdot xH_2O$, 99.95% trace metals basis), erbium(III) acetate hydrate ($Er(CH_3COO)_3 \cdot xH_2O$, 99.9% trace metals basis), oleic acid (technical grade, 90%), 1-octadecene

(technical grade, 90%), ammonium fluoride (NH_4F, ACS reagent, ≥98.0%), sodium hydroxide (NaOH, BioXtra, ≥98% (acidimetric), pellets (anhydrous)), methanol (for HPLC, ≥99.9%), cyclohexane (ACS reagent, ≥99%), OTA, ochratoxin B (OTB), zearalenone (ZEA), aflatoxin B1 (AFB1), sulfuric acid (ACS reagent, 95.0–98.0%), (3-aminopropyl)trimethoxysilane (APTMS, 97%), glycine (ACS reagent, ≥98.5%), Tris base, and *N*-hydroxysuccinimide (NHS, 98%) were purchased from Sigma-Aldrich. 1,2-Dipalmitoyl-sn-glycero-3-phosphoethanolamine-*N*-[methoxy(polyethylene glycol)-2000] (mPEG) and 1,2-distearoyl-sn-glycero-3-phosphoethanolamine-*N*-[carboxy(polyethylene glycol)-2000] (DSPE-PEG-carboxylic acid) were purchased from Avanti Polar Lipids (Alabaster, AL, USA). Ethanol (HPLC grade) was purchased from Duksan (Ansan, South Korea). 1-Ethyl-3-(3-dimethylaminopropyl) carbodiimide hydrochloride (EDC) and borate buffer were obtained from Thermo Fisher Scientific (Waltham, MA, USA). Deoxyribonucleic acid (DNA) oligonucleotides (BHQ1-labeled and Cy5-labeled) were custom-made at Xenotech (Daejeon, South Korea). Hydrogen peroxide (35% w/w aq. soln., stab.) was purchased from Alfa Aesar. PDMS (SYLGARD 184) was purchased from Dow Corning (USA).

2.2. Synthesis of $NaYF_4:Yb^{3+},Er^{3+}$ nanoparticles

$NaYF_4:Yb^{3+},Er^{3+}$-based UCNPs were synthesized using the liquid-solid solution solvothermal method according to previously reported procedures (Park et al., 2012). In brief, $Y(CH_3COO)_3 \cdot xH_2O$ (0.78 mmol), $Yb(CH_3COO)_3 \cdot xH_2O$ (0.20 mmol), and $Er(CH_3COO)_3 \cdot xH_2O$ (0.02 mmol) were mixed with 8 mL of oleic acid and 15 mL of 1-octadecene in a 50 mL flask under a nitrogen atmosphere. The mixed solution was heated to 160 °C, which was maintained for 30 min with stirring, and then cooled to room temperature. Ten milliliters of NaOH (0.25 M) and NH_4F (0.4 M) in methanol was injected into the solution, which was then stirred for 30 min

at room temperature to obtain UCNPs. The solution was heated to 100 °C and maintained for 30 min to evaporate methanol, and then the temperature was increased to 300 °C and maintained for 1 h. The synthesized UCNPs in solution were washed with ethanol using a centrifuge (9500 rpm for 20 min) three times, then resuspended in cyclohexane.

2.3. Synthesis of carboxy PEG-capped UCNPs

Carboxylation of UCNPs was performed as previously reported (Jo et al., 2018). UCNPs in chloroform (2 mg mL^{-1}, 5 mL) were mixed with solutions of 3 mg mL^{-1} mPEG and 1 mg mL^{-1} DSPE-PEG-carboxylic acid in chloroform, and the mixture was stirred for 30 min at room temperature. To evaporate chloroform, the UCNP-containing solution was heated in a vacuum oven at 65 °C for 1 h. Then, 10 mL of deionized water (DW) was added to the fully dried UCNPs. After filtration with a 0.2 µm cellulose acetate syringe filter, the carboxy PEG-capped UCNPs were washed three times with DW using a centrifuge (9500 rpm for 20 min). Finally, the carboxy PEG-capped UCNPs were resuspended and stored in DW.

2.4. Fabrication of Au/UCNPs and UCNPs on PDMS substrates for aptasensors

Glass slides (15 mm × 15 mm) were treated using piranha solution (H_2SO_4:H_2O_2=3:1) and washed with DW. Then, a self-assembled monolayer (SAM) of APTMS was formed on the glasses by exposure to an APTMS solution (4% APTMS in ethanol) for 2 h; the SAM of APTMS resulted in an aminated glass surface. Fifty microliters of UCNP solution (0.05 mg mL^{-1} in DW) was dropped onto the aminated glass and dried at 40 °C in an oven. Glancing angle deposition of Au thin films was performed on the UCNP/glass samples using an e-beam evaporator; the deposition thickness and angle were 40 nm and 60°, respectively. Note that this Au deposition step was skipped for the fabrication of UCNPs on the PDMS substrate. Next, a mixture of PDMS and curing agent (ratio of 10:1) was poured onto the Au-deposited

UCNP/glass slides, which were placed in Petri dishes. After extracting bubbles from the PDMS by a vacuum pump, the PDMS was cured at 65 °C in an oven for 2 h. Finally, the PDMS was cut to a size larger than the glass slide, then detached from the Petri dishes and glass slides, resulting in the formation of a rectangular vessel of PDMS with Au/UCNPs embedded at the surface. (For the fabrication of bare UCNP-embedded PDMS, the same procedures were performed without the deposition of Au.)

2.5. Fabrication of UCNPs on glass substrate for aptasensors

The deposition of UCNPs on a glass substrate for the fabrication of aptasensors was performed following the same procedure as that used for the fabrication of Au/UCNPs on PDMS, although Au thin films were not deposited.

2.6. Upconversion emission measurement

The UCL emission spectra were measured using a customized microscope (Olympus BX43, Tokyo, Japan) equipped with a spectrometer (SR-500i-A, Andor Tech, USA), charged coupled device (CCD) camera (DV420A-OE, Andor Tech, USA), and 980-nm laser (SSL-LM-980-600-D, Shanghai Sanctity Laser Technology, Shanghai, China) as an excitation source for the UCNPs.

2.7. Aptamer functionalization on Au/UCNPs on PDMS, UCNPs on PDMS, and UCNPs on glass

The aptamers used in this work were amine- and quencher-modified at each end (amino-AAA AAG CAT CTG ATC GGG TGT GGG TGG CGT AAA GG-black hole quencher-1 (BHQ1)). The sequence of the aptamer can specifically bind with OTA (Jo et al., 2018). To prepare Au/UCNPs on PDMS substrates as biosensors, the aptamers were functionalized onto the open surface of the carboxylated UCNPs, where they were not covered by the Au nanocaps, located in

the vessel of the PDMS substrate. Notably, the functionalization of UCNPs on PDMS and UCNPs on glass was performed following the same procedure as that of Au/UCNPs on PDMS. However, for UCNPs on glass, the PDMS vessel was prepared separately. First, EDC/NHS coupling reactions (0.1 M EDC in DW and 0.025 M NHS in DW were used) were performed on the Au/UCNPs for 15 min to activate the carboxylated UCNPs and functionalize the amino-aptamer. A simple washing step was carried out by spraying DW onto the samples using a squeeze bottle. Then, 100 µM aptamer solution (in 10 mM HEPES buffer, pH 7.2) was dropped onto the Au/UCNPs on PDMS and incubated for 3 h. Another washing step was performed using 2% SDS and DW in turn. Next, a blocking process for the activated functional groups on the surface was performed by exposure to glycine (20 mM in HEPES) for 30 min and 50 mg mL^{-1} Tris for 30 min. Finally, a washing process was performed using DW.

2.8. OTA detection using Au/UCNPs functionalized with aptamers on PDMS

After functionalization, a 10 mM borate buffer solution (pH 8.5) containing 4 mM KCl (this solution was used in all experiments for OTA detection as the binding buffer) was injected onto the PDMS vessels where aptamer-functionalized Au/UCNPs were partially embedded. Cover glasses were used to partially cover the PDMS vessels containing the borate buffer solution and, at the same time, fully cover the pathway of the 980-nm laser light. The roles of cover glass were to ensure a uniform thickness of the buffer solution and minimize the evaporation of the buffer solution during assays. Before OTA detection, the aptamer-functionalized Au/UCNPs on PDMS were incubated at 70 °C in an oven for 1 h to stretch any unintentionally folded aptamers. OTA detection was carried out by comparing measured UCL spectra from the injection of control solution (DW) and OTA solution (in DW) into the borate buffer solution contained in the PDMS vessels. Various concentrations of OTA were used for detection: final concentrations of 0.1, 1,

10, 100, and 1000 ng mL^{-1}. The UCL emission spectra were measured 30 min after injection of the control or OTA solution. To minimize evaporation of the borate buffer solution during assays, the spectrometer chamber was kept at a humid environment using wet disposable wipers (KIMTECH).

2.9. Regeneration of aptamer-functionalized Au/UCNPs on PDMS

Regeneration of aptamers after OTA detection was carried out by injecting 10% methanol (in DW) onto the aptamer-functionalized Au/UCNPs in PDMS vessels and incubating at 70 °C for 30 min (Park et al., 2014). Then, the aptamer-functionalized Au/UCNPs were washed with DW and stored in 10 mM borate buffer (pH 8.5). Before reuse of the regenerated aptamer-functionalized Au/UCNPs on PDMS, they were incubated at 70 °C in an oven for 1 h to stretch unintentionally folded aptamers, then used to detect OTA again.

3. RESULTS AND DISCUSSION

The fabrication of aptamer-functionalized Au/UCNPs on PDMS as a solid-phase, single-step biosensor is described in **Fig. 1a,b**. In brief, a solution containing UCNPs (characterized in detail in **Fig. S1**) was drop-cast onto a glass substrate and dried (**Fig. 1a**). Scanning electron microscopy (SEM) imaging of the resulting UCNP-coated glass substrate demonstrated the formation of a UCNP monolayer (**Fig. S2a,b**). Then, Au was deposited using an e-beam evaporator to form Au nanocaps on UCNPs (**Fig. S2c**), which resulted in an approximately four-fold UCL enhancement (**Fig. S3**), which was ascribed to the deposited Au (Bang et al., 2017; Hinamoto et al., 2017). For transfer of Au/UCNPs onto a solid substrate and the conversion of their direction, PDMS was poured onto Au/UCNPs on the glass substrate and cured until hardening. The role of PDMS was to serve as a solid substrate for Au/UCNPs, thus facilitating

the fabrication of solid-phase biosensors; PDMS effectively immobilized Au/UCNPs by physically surrounding them and leading to stable operation during target detection. Au/UCNPs partially embedded in PDMS were finally obtained by PDMS detachment. This transfer process, based on PDMS, was necessary because the area where the UCNPs were not covered by Au nanocaps needed to be exposed outside PDMS to functionalize the aptamers on the UCNPs. Besides, the cavity produced by the above detachment was used as an assay vessel. After detachment, the embedded Au/UCNPs were observed by SEM (**Fig. S4a,b**), leaving the Au film deposited on a glass substrate without the transferred Au/UCNPs (**Fig. S4c,d**). For OTA-binding aptamer functionalization (amine- and BHQ1-modification at each end), EDC/NHS coupling was performed to covalently attach the amine at the end of the aptamer to carboxylated UCNPs (**Fig. 1b**).

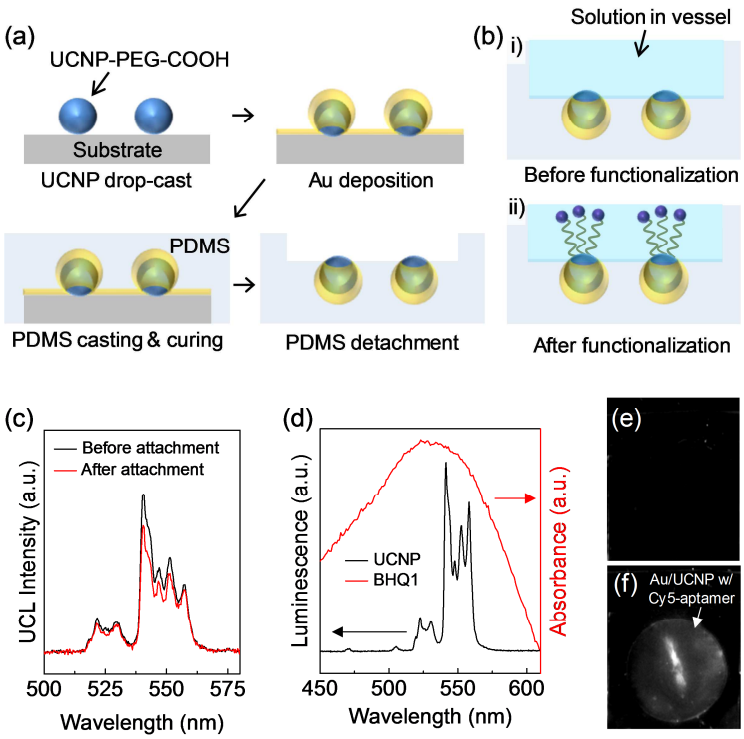

Figure 1. (a,b) Schematic illustration of the fabrication process for Au/UCNPs on PDMS substrate functionalized with quencher-labeled aptamers as a solid-phase aptasensor. (c) UCL spectra before and after aptamer (labeled with BHQ1) functionalization. (d) Absorption spectrum of quencher (BHQ1) and UCL spectrum of UCNPs. Fluorescence images acquired (e) before and (f) after aptamer (labeled with Cy5) functionalization.

The above aptamer functionalization was confirmed by reduction in the UCL of the UCNPs, with the corresponding observations conducted under wet conditions as described in **Fig. 1b i) and ii)**. Importantly, the sample was not moved during aptamer functionalization to exactly measure the extent of UCL reduction of the UCNPs (determined as 17.5%; **Fig. 1c**). The reasons for the reduction were expected because of the attachment of BHQ1-labeled aptamers, resulting in i) adsorption of emitted light from UCNPs by BHQ1 (**Fig. 1d**), and ii) quenching phenomenon, to some degree, caused by unintentionally folded aptamers. In addition to functionalization with BHQ1-labeled aptamers, those with Cy5-labeled aptamers were also performed in the same way to directly observe attachment by imaging the fluorescence of Cy5, which is more detectable than the absorbance of BHQ1 or DNA (**Fig. 1e,f**). After functionalization of the Cy5-labeled aptamers on Au/UCNPs, a fluorescence signal was observed only from the area where Au/UCNPs had been transferred onto PDMS after Cy5-aptamer attachment (**Fig. 1e,f**). It should be noted that although the Cy5-aptamer solution covered the entire PDMS vessel during the attachment, attachment was ultimately observed only in regions where Au/UCNPs were present. These results indicated that EDC/NHS coupling reactions on the Au/UCNPs allowed for successful aptamer attachment.

The working principle of solid-phase, single-step biosensors composed of UCNP (donor) and BHQ1 (acceptor) linked by an aptamer, as described in **Fig. S5**, is based on UCL quenching of UCNPs via FRET (Clapp et al., 2004; Medintz et al., 2006; Bednarkiewicz et al., 2010). The above quenching is caused by aptamer folding after target binding, as this folding results in a

shortened distance between the UCNP and the quencher with overlapped emission and absorption spectra, respectively. In detail, FRET efficiency is inversely proportional to the sixths power of the donor-to-acceptor distance, as described below (**Eq. 1, 2**).

$$\text{FRET efficiency} = \frac{1}{1+(\frac{r}{R_0})^6}, \quad (1)$$

$$R_0^6 = 8.79 \times 10^{-28}\, mol \times (n^{-4}\kappa^2\Phi_D J), \quad (2)$$

where r is the donor-to-acceptor distance, R_0 is the Förster distance, n is the refractive index of the surrounding medium, κ^2 is the relative orientation between donor emission and acceptor absorption dipoles, Φ_D is the quantum yield of the donor, and J is the degree of spectral resonance between the two species. Hence, aptamer folding induced by target-aptamer binding results in a shortening of the distance (r) between UCNPs and quenchers (BHQ1), thereby facilitating UCL quenching. Thus, the extent of UCL quenching can be used to quantify the concentration of a target in solution. For a model study, OTA, one of the most abundant mycotoxins observed in contaminated food, was chosen as the target (Jo et al., 2018).

Solid-phase single-step biosensor platforms based on a glass substrate were fabricated by immobilization of UCNPs on a slide glass followed by attachment of quencher (BHQ1)-modified aptamers (**Fig. 2a,b**). The absorbance of the BHQ1 quencher overlaps with the emission spectrum of UCNPs, meeting the requirements for FRET (**Fig. 1c,d**). Before OTA solution injection, the solid-phase aptasensor exposed to binding buffer (10 mM borate buffer (pH 8.5) with 4 mM KCl) was heated at 70 °C for 30 min to stretch any unintentionally folded aptamers. The adopted binding buffer conditions, based on the results of our previous work, were optimal for OTA detection (Jo et al., 2018). A schematic illustration of UCL measurement for OTA

detection is shown in **Fig. S6**. A relatively low UCL quenching efficiency of ~17% was observed in the presence of 1 μg mL^{-1} OTA (**Fig. 2c**), as compared to values of ~35% previously reported for single-step solution-phase OTA aptasensors (Jo et al., 2018). Quenching efficiency was calculated using **Eq. 3**.

$$\text{Quenching efficiency (\%)} = \frac{I_{initial} - I_{detection}}{I_{initial}} \times 100, \quad (3)$$

where I_{initial} and $I_{\text{detection}}$ are the peak areas of the UCL spectrum before and after OTA injection, respectively. The reason for such low sensitivity toward OTA was ascribed to the fact that the area where the aptamer-BHQ1 can functionalize UCNPs was reduced because of contact with glass (**Fig. 2a**). Considering that upconverted light can be emitted from the entire UCNP surface, aptamer functionalization of this limited area results in low sensitivity, which is a critical disadvantage for sensing applications despite the potential for portable biosensor usage.

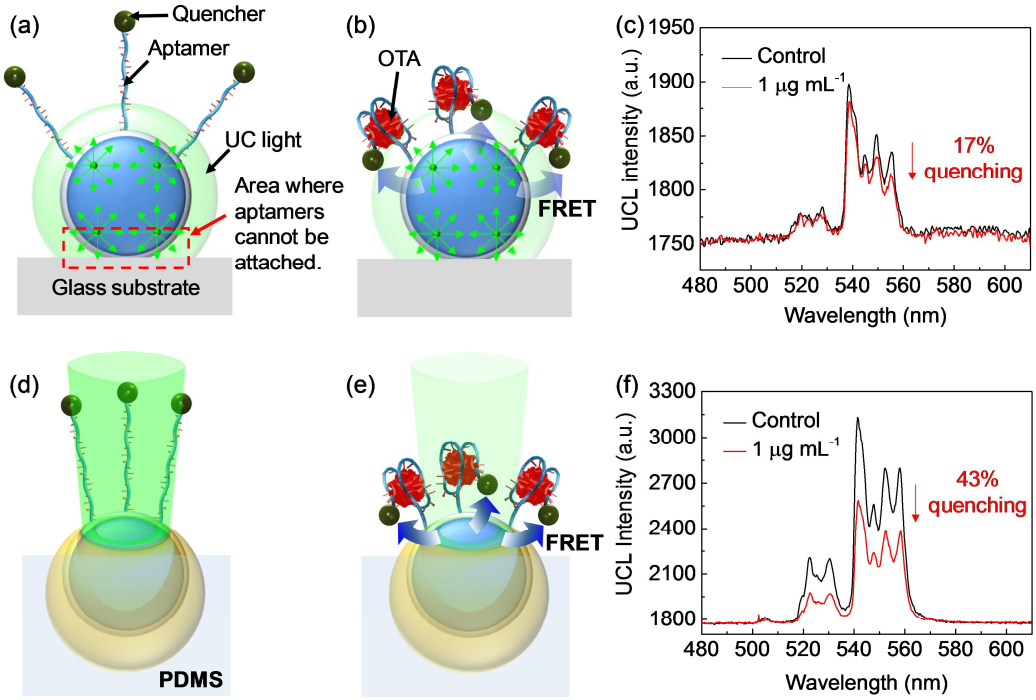

Figure 2. Schematic illustrations of OTA detection using aptamer (labeled with a quencher)-functionalized bare UCNPs on a glass substrate based on FRET-induced quenching: (a) before and (b) after OTA detection. (c) UCL spectra acquired before and after OTA detection for aptamer (labeled with a quencher)-functionalized bare UCNPs. The same schematic illustrations for the case of Au/UCNPs on PDMS instead of bare UCNPs on glass: (d) before and (e) after OTA detection. (f) UCL spectra acquired before and after OTA detection for Au/UCNPs on PDMS. The incubation time for OTA-aptamer binding was 30 min for each aptasensor.

To solve this problem, the Au/UCNPs were introduced to the solid-phase aptasensor (**Scheme 1**). Previous works have shown that Au/UCNPs can strongly emit upconverted light from a restricted UCNP area, near the Au nanocap edge (Bang et al., 2017; Hinamoto et al., 2017). Moreover, localized surface plasmon resonance (LSPR) of Au nanocaps on UCNPs enhances the UCL of UCNPs. Thus, aptamer functionalization on the restricted area of Au/UCNPs on a PDMS substrate could be a promising way of fabricating solid-phase biosensors, as aptamer-BHQ1 can fully cover the UCNP area capable of emitting upconverted light to result in effective quenching of upconverted light from Au/UCNP by BHQ1.

The performance of Au/UCNPs functionalized with BHQ1-labeled aptamers on the PDMS substrate (hereafter denoted as Au/UCNP-based solid-phase aptasensor) was evaluated by exposure to OTA (**Fig. 2d,e**). Before OTA solution injection, the Au/UCNP-based solid-phase aptasensor containing binding buffer in the PDMS vessel (i.e., in the empty volume created by glass slide removal) was heated at 70 °C for 30 min to stretch any unintentionally folded aptamers. The Au/UCNP-based solid-phase aptasensor showed UCL quenching efficiency of ~42% for 1 μg mL^{-1} OTA (**Fig. 2f**), which significantly exceeded the value obtained in the case of UCNPs on glass substrate (~17%) (**Fig. 2c**). More comparisons with solid-phase aptasensors presented in this work are shown in **Fig. S7**. As illustrated in **Scheme 1**, the high quenching efficiency of the Au/UCNP-based solid-phase aptasensor compared with that of the UCNP-based solid-phase ones (UCNPs on both glass and PDMS) was attributed to the focusing of UCL at the specific area where aptamer functionalization occurred.

The Au/UCNP-based solid-phase aptasensor was then employed to detect various OTA final concentrations of 0.1–1000 ng mL^{-1}, as shown in **Fig. 3a**. UCL measurement was performed by sequential injection of OTA solutions from low to high concentrations into the binding solution without any sample movement. The incubation time for OTA-aptamer binding equaled 30 min for each concentration. As a result, an increase in FRET-attributable UCL quenching was observed with increasing OTA concentration (**Fig. 3a**).

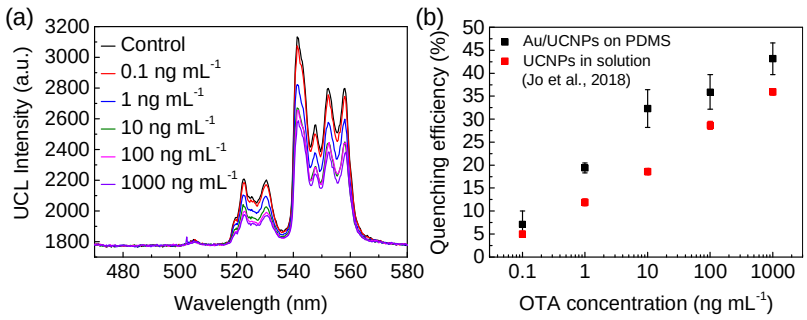

Figure 3. (a) OTA detection using Au/UCNP-based solid-phase aptasensor within the range of 0.1–1000 ng mL^{-1}. (b) Comparison of the performance of solid-phase and solution-phase biosensors: UCNP on PDMS and Au/UCNP on PDMS for solid-phase and UCNPs dispersed in solution for solution-phase using the results adopted from the previous work reported by our group (Jo et al., 2018).

Comparisons of the quenching efficiencies of Au/UCNP-based solid-phase and UCNP-based solution-phase aptasensors are presented in **Fig. 3b**. Note that the results of OTA detection by the UCNP-based solution-phase sensor are taken from the work of Jo et al. (2018). The sensing performances of solid-phase (Au/UCNP-based) (black dots in **Fig. 3b**) and solution-phase aptasensors (red dots in **Fig. 3b**) (Jo et al., 2018) were compared. Sensitivity of the former aptasensor toward OTA was slightly higher than that of the latter within the linear range of 0.1–1000 ng mL^{-1}, and the limit of detection (LOD), which is the lowest OTA concentration required to produce a signal greater than three times the standard deviation of the noise level (S/N = 3), of the solid-phase aptamer was calculated as 0.022 ng mL^{-1} (**Fig. S8**). A detailed comparison of our solid-phase biosensors with those previously reported in literature is given in **Table S1**. The higher sensitivity of the solid-phase aptasensor compared to that of solution-phase ones was expected because of the following two reasons. (a) The enhanced emission properties of UCNPs owing to the LSPR of Au nanocaps on UCNPs are responsible for the enhanced sensitivity, as the quantum yield of the donor (Φ_D) increased the FRET efficiency according to **Eq. 2** (Clapp et

al., 2004; Medintz et al., 2006; Bednarkiewicz et al., 2010; Wiesholler et al., 2018). (b) The LSPR due to Au nanocap presence might also lead to plasmon-assisted enhancement of FRET during OTA detection (Aissaoui et al., 2017; Anderson et al., 2019; Bohlen et al., 2019; Cao et al., 2019). Hence, the Au/UCNP-based solid-phase aptasensor showed a comparable or even higher sensitivity than that of the solution-phase one. Furthermore, the selectivity of the aptasensor was also evaluated toward OTB, ZEA, and AFB1 (**Fig. S9**), confirming that the aptasensor could selectively detect only OTA.

The reusability of portable biosensors is also an important factor for POC testing; therefore, the Au/UCNP-based solid-phase aptasensor was evaluated as a regenerable biosensor. The aptamer can be regenerated under specific conditions such as elevated temperature or exposure to HCl or NaOH solutions (Prabhakar et al., 2011; Ye et al., 2012; Park et al., 2014). Among the various regeneration techniques for the aptamers, the elevated temperature method, which was reported in a previous work from our group (Park et al., 2014), was adopted to regenerate our solid-phase aptasensors. The detailed procedure for the regeneration process is described in the Experimental section. **Fig. 4** shows the results of OTA (1 μg mL^{-1}) detection and regeneration for three cycles (raw data are shown in **Fig. S10**). Although there was a slight deviation at each cycle, apparent detection and regeneration tendencies were observed. Thus, the Au/UCNP-based solid-phase biosensor is a potential platform for reusable POC testing.

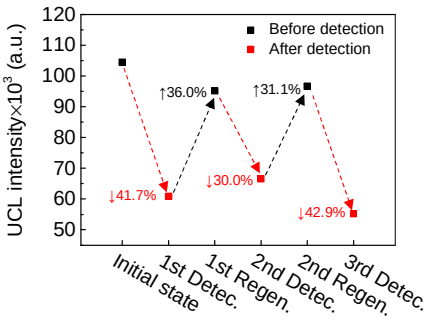

Figure 4. Regeneration and reuse of Au/UCNP-based solid-phase aptasensor by exposure to 70 °C for 1 h.

4. CONCLUSIONS

In this paper, we demonstrated a solid-phase, single-step aptasensor based on Au nanocap-supported UCNPs functionalized with quencher-labeled aptamers on a PDMS substrate. The Au/UCNP-based solid-phase aptasensor was used to detect OTA within the range of 0.1–1000 ng mL^{-1} on the basis of quenching of the UCL of UCNPs caused by FRET between the UCNPs and quencher. The role of the Au nanocaps on the UCNPs was to restrict the strong UCNP emission of upconverted light to a specified area due to LSPR phenomenon. Functionalization of aptamers on this specified area with strong upconverted light emission led to a sensing performance (detection range: 0.1–1000 ng mL^{-1}; LOD: 0.022 ng mL^{-1} within 30 min in a single step) comparable to that of solution-phase biosensors. Moreover, the Au/UCNP-based solid-phase aptasensor showed potential for reusability for three cycles by exposure to an elevated temperature. As a solid-phase biosensor, this aptasensor could afford the advantages of portability, ease of washing, and reusability, which could therefore pave the way to developing a highly effective platform for POC testing.

ACKNOWLEDGMENT

This work was financially supported by grants from the Global Research Laboratory (GRL) Program (NRF-2013K1A1A2A02050616); the Mid-Career Researcher Program (NRF-2017R1A2B3010816) through a National Research Foundation grant funded by the Ministry of Science, ICT, and Future Planning; BioNano Health-Guard Research Center funded by the Ministry of Science and ICT (MSIT) of Korea as a Global Frontier Project (Grant number H-GUARD_2013M3A6B2078950); and GIST Research Institute (GRI) grant funded by the GIST in 2019.

Conflict of interests

The authors declare no conflict of interests.

REFERENCES

Aissaoui, N., Moth-Poulsen, K., Käll, M., Johansson, P., Wilhelmsson, L.M., Albinsson, B., 2017. Nanoscale 9, 673–683.

Anderson, N.T., Ren, S., Chao, J., Dinolfo, P.H., Wang, X., 2019. ACS Appl. Nano Mater. 2, 5563–5572.

Bang, D., Jo, E.-J., Hong, S., Byun, J.-Y., Lee, J.Y., Kim, M.-G., Lee, L.P., 2017. Nano Lett. 17, 6583–6590.

Bednarkiewicz, A., Nyk, M., Samoc, M., Strek, W., 2010. J. Phys. Chem. C 114, 17535–17541.

Bohlen, J., Cuartero-González, Á., Pibiri, E., Ruhlandt, D., Fernández-Domínguez, A.I., Tinnefeld, P., Acuna, G.P., 2019. Nanoscale 11, 7674–7681.

Cao, J., Zhang, H., Liu, X., Zhou, N., Pi, X., Li, D., Yang, D., 2019. J. Phys. Chem. C 123, 23604–23609.

Clapp, A.R., Medintz, I.L., Mauro, J.M., Fisher, B.R., Bawendi, M.G., Mattoussi, H., 2004. J. Am. Chem. Soc. 126, 301–310.

Doughan, S., Han, Y., Uddayasankar, U., Krull, U.J., 2014. ACS Appl. Mater. Interfaces 6, 14061–14068.

Doughan, S., Uddayasankar, U., Krull, U.J., 2015. Anal. Chim. Acta 878, 1–8.

Gubala, V., Harris, L.F., Ricco, A.J., Tan, M.X., Williams, D.E., 2012. Anal. Chem. 84, 487–515.

Guan, W., Zhou, W., Lu, J., Lu, C., 2015. Chem. Soc. Rev. 44, 6981–7009.

Gu, B., Zhang, Q., 2018. Adv. Sci. 5, 1700609.

Han, Y., Noor, M.O., Sedighi, A., Uddayasankar, U., Doughan, S., Krull, U.J., 2017. Langmuir 33, 12839–12858.

Hinamoto, T., Takashina, H., Sugimoto, H., Fujii, M., 2017. J. Phys. Chem. C 121, 8077–8083.

Jo, E.-J., Byun, J.-Y., Mun, H., Bang, D., Son, J.H., Lee, J.Y., Lee, L.P., Kim, M.-G., 2018. Anal. Chem. 90, 716–722.

Luppa, P.B., Müller, C., Schlichtiger, A., Schlebusch, H., 2011. Trac-Trends Anal. Chem. 30, 887–898.

Medintz, I.L., Clapp, A.R., Brunel, F.M., Tiefenbrunn, T., Tetsuo Uyeda, H., Chang, E.L., Deschamps, J.R., Dawson, P.E., Mattoussi, H., 2006. Nat. Mater. 5, 581–589.

Nayak, S., Blumenfeld, N.R., Laksanasopin, T., Sia, S.K., 2017. Anal. Chem. 89, 102–123.

Prabhakar, N., Matharu, Z., Malhotra, B.D., 2011. Biosens. Bioelectron. 26, 4006–4011.

Park, Y.I., Kim, H.M., Kim, J.H., Moon, K.C., Yoo, B., Lee, K.T., Lee, N., Choi, Y., Park, W., Ling, D., Na, K., Moon, W.K., Choi, S.H., Park, H.S., Yoon, S.-Y., Suh, Y.D., Lee, S.H., Hyeon, T., 2012. Adv. Mater. 24, 5755–5761.

Park, J.-H., Byun, J.-Y., Mun, H., Shim, W.-B., Shin, Y.-B., Li, T., Kim, M.-G., 2014. Biosens. Bioelectron. 59, 321–327.

Quesada-González, D., Merkoçi, A., 2018. Chem. Soc. Rev. 47, 4697–4709.

Sedlmeier, A., Gorris, H.H., 2015. Chem. Soc. Rev. 44, 1526–1560.

Samorì, P., Biscarini, F., 2018. Chem. Soc. Rev. 47, 4675–4676.

Vashist, S.K., Luppa, P.B., Yeo, L.Y., Ozcan, A., Luong, J.H.T., 2015. Trends Biotechnol. 33, 692–705.

Wiesholler, L.M., Genslein, C., Schroter, A., Hirsch, T., 2018. Anal. Chem. 90, 14247–14254.

Wood, C.S., Thomas, M.R., Budd, J., Mashamba-Thompson, T.P., Herbst, K., Pillay, D., Peeling, R.W., Johnson, A.M., McKendry, R.A., Stevens, M.M., 2019. Nature 566, 467–474.

Xu, Sai, Xu, Shihan, Zhu, Y., Xu, W., Zhou, P., Zhou, C., Dong, B., Song, H., 2014. Nanoscale 6, 12573–12579.

Ye, B.-F., Zhao, Y.-J., Cheng, Y., Li, T.-T., Xie, Z.-Y., Zhao, X.-W., Gu, Z.-Z., 2012. Nanoscale 4, 5998.

Ye, W.W., Tsang, M.-K., Liu, X., Yang, M., Hao, J., 2014. Small 10, 2390–2397.

Ye, F., Zhao, Y., El-Sayed, R., Muhammed, M., Hassan, M., 2018. Nano Today 18, 103–123.

Zheng, W., Huang, P., Tu, D., Ma, E., Zhu, H., Chen, X., 2015. Chem. Soc. Rev. 44, 1379–1415.

Graphical abstract

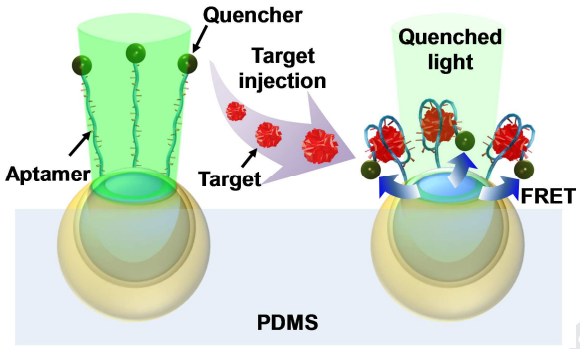

Highlight

- Concept & design of solid-phase, single-step biosensors were demonstrated
- Fabrication based on Au nanocap-supported upconversion nanoparticles on PDMS
- Quencher-labeled aptamers functionalized onto exposed Au/nanoparticle area
- Sensitivity toward ochratoxin A was comparable to that of solution-phase sensor
- Reusability of solid-phase single-step aptasensor was successful via heat treatment

Author Contribution Statement

Kihyeun Kim: Conceptualization, Methodology, Validation, Formal Analysis, Investigation, Visualization, Writing – Original Draft, Writing – Review & Editing

Eun-Jung Jo: Methodology, Formal Analysis, Investigation, Writing – Original Draft

Ki joong Lee: Methodology, Formal Analysis, Investigation

Jiyoon Park: Methodology, Investigation

Gun Young Jung: Investigation, Writing – Review & Editing

Yong-Beom Shin: Formal Analysis, Investigation, Writing – Review & Editing

Luke P. Lee: Conceptualization, Writing – Review & Editing, Funding acquisition, Supervision, Project Administration

Min-Gon Kim: Conceptualization, Writing – Review & Editing, Funding acquisition, Resources, Supervision, Project Administration

Declaration of interests

☒ The authors declare that they have no known competing financial interests or personal relationships that could have appeared to influence the work reported in this paper.

☐The authors declare the following financial interests/personal relationships which may be considered as potential competing interests: